Macromolecules
ARTICLE

Macromolecules **2010**, *43*, 8985–8992 **8985**
DOI: 10.1021/ma101721d

Chain-Length Dependence of the Segmental Relaxation in Polymer Melts: Molecular Dynamics Simulation Studies on Poly(propylene oxide)

A. Bormuth, P. Henritzi, and M. Vogel*

Institut für Festkörperphysik, Technische Universität Darmstadt, 64289 Darmstadt, Germany

Received July 29, 2010; Revised Manuscript Received September 27, 2010

ABSTRACT: Performing molecular dynamics simulations for an all-atom force field, we study the segmental or, equivalently, α relaxation of poly(propylene oxide) chains consisting of $N = 2-100$ monomer units. In particular, we analyze the dependence of the α relaxation on molecular weight and temperature on the basis of incoherent intermediate scattering functions. For all studied chain lengths N, the temperature dependence is well described by a Vogel−Fulcher−Tammann behavior and time−temperature superposition is obeyed at sufficiently low temperatures T. When the molecular weight increases, time scale and stretching of the α relaxation smoothly increase until they saturate at $N = 30-40$, where the characteristic ratio reaches the limiting value C_∞ and, hence, the chains start to show Gaussian conformation. The temperature-dependent α relaxation times collapse onto a master curve in a fragility plot, indicating that the high-temperature fragility of the model polymer is independent of the degree of polymerization. We determine to which extent the observed dependence of the segmental relaxation time on T and N can be traced back to excess free volume near chain ends within free-volume theory.

Introduction

Polymer dynamics is of enormous interest for fundamental and applied science, including the request for improved material properties. One important feature is the slowing of the segmental or, equivalently, α relaxation of polymer melts approaching the glass-transition temperature T_g. Two key features characterize the α relaxation: its time dependence differs from a single exponential, and its temperature dependence deviates from an Arrhenius law. In particular, in the monomeric regime, these properties and, thus, the glass-transition temperature strongly depend on the molecular weight. Therefore, it is important for a fundamental understanding of melt behavior to ascertain the features of segmental dynamics as a function of the number of monomeric units N.

Fox and Flory[1,2] proposed a time-honored empirical equation for the molecular-weight dependence of the glass-transition temperature:

$$T_g(N) = T_{g,\infty} - \frac{K}{N} \tag{1}$$

Such behavior can be rationalized when assuming that polymers of different chain length N exhibit the same free volume at T_g and considering that chains ends contribute excess free volume. Later, other relations were put forward.[3,4] For example, Dobkowski suggested[5]

$$T_g(N) = T_{g,\infty} - \frac{K}{N + N^*} \tag{2}$$

In eqs 1 and 2, $T_{g,\infty}$ is the glass-transition temperature for infinite chain length. K and N^* are empirical constants.

While several experimental studies[6−10] confirm the smooth increase of $T_g(N)$ predicted by these relations, others[11,12] reported that the increase of $T_g(N)$ is not continuous, but rather exhibits three linear regimes. These regimes were assigned to (I) simple liquid, (II) oligomer, and (III) polymer; i.e., they were argued to reflect effects of chain connectivity and entanglements on the segmental relaxation. Specifically, the crossover between regimes I and II was proposed to mark the size of the Rouse unit N_R and the crossover between regimes II and III was suggested to occur at N_E, the number of monomers between entanglements.[11] A list of all symbols can be found in the Appendix. Thus, on the basis of these regimes, if existent, it may be possible to determine N_R and N_E and, hence, to shed light on the intriguing question of when does a molecule become a polymer. However, other workers challenged this view and put forward that $T_g(N)$ does not saturate at the entanglement length N_E, but rather at N_G, being the minimum chain length for which chain conformation obeys Gaussian statistics.[9,13]

Molecular dynamics simulations (MDS) proved a versatile tool to investigate polymer dynamics. Various coarse-grained[14,15] and all-atom[16,17] models were used in MDS of polymer melts. Excellent review articles give nice overviews over different simulation techniques.[18,19] While experimental studies on the molecular-weight dependence of polymer dynamics may suffer from a polydispersity of the polymer and from a presence of impurities, monodisperse and pure systems can be investigated in computational work. Thus, MDS yield valuable information in the accessible time window, which nowadays typically extends from about 10^{-15} to 10^{-7} s, provided the employed force field enables an appropriate description of the polymer. A number of workers exploited this potential and performed MDS to analyze the dependence of polymer dynamics on the degree of polymerization for different types of models, ranging from freely jointed chains to chemically realistic force fields.[20−34] However, MDS studies on the molecular-weight dependence of the segmental relaxation are still rare.[26,28,32,34]

Here, MDS are performed for a chemically realistic all-atom model of poly(propylene oxide) (PPO). Since PPO is capable to dissolve salts, it is a promising candidate for use in polymer electrolytes.[35] In previous works,[36−38] we used NMR spectroscopy

*To whom correspondence should be addressed. E-mail: michael.vogel@physik.tu-darmstadt.de.

Published on Web 10/15/2010

Table 1. Studied Systems

N	no. of molecules	no. of atoms
2	200	3800
3	128	3712
4	96	3744
6	64	3776
9	48	4272
12[a]	32[a]	3808[a]
16	24	3816
18	22	3938
20	20	3980
22	18	3942
24	16	3824
36	12	4308
48	8	3832
100	4	3996

[a] These data were reported in previous work.[39]

to characterize PPO dynamics in the presence and absence of salts. In addition, we utilized MDS to study the torsional and segmental motions of a PPO melt composed of chains of length $N = 12$.[39] In the present contribution, our MDS work is extended to the range $N = 2-100$. The focus is on an analysis of the segmental relaxation as a function of temperature T and chain length N. In particular, we investigate how the degree of polymerization affects time scale and nonexponentiality of the α relaxation. In this way, we analyze whether different regimes can be distinguished. These results are discussed in the context of the chain-length dependence of the characteristic ratio C to search for correlations between dynamical and structural properties. Moreover, we determine the free volume as a function of N and T to ascertain whether the dependence of the segmental relaxation time τ on these parameters can be traced back to excess free volume in the vicinity of chain ends within free-volume theory.[40−42] The molecular-weight dependence of the Rouse dynamics of the PPO model will be addressed in future work.

Methods

We simulate atactic PPO chains $CH_3-O-[CH_2-CH(CH_3)-O]_{N-1}-CH_3$. To specify the chain length of the molecules, we use the nomenclature PPO_N. All studied systems contain about 4000 atoms so that the number of molecules decreases from 200 for PPO_2 to 4 for PPO_{100} (see Table 1). We employ a classical chemically realistic all-atom force field of the form[43]

$$V(\{\vec{r}\}) = \sum_{\text{bonds}} V^{\text{bo}}(r_{ij}) + \sum_{\text{angles}} V^{\text{an}}(\theta_{ijk}) + \sum_{\text{dihedrals}} V^{\text{tor}}(\phi_{ijkl}) + V^{\text{nb}}(\{\vec{r}\}) \quad (3)$$

Here, $\{\vec{r}\}$ is the set of all particle coordinates. The bonded interactions include potentials for bond stretching, bond bending, and torsional motion of dihedrals. The nonbonded interactions V^{nb} comprise van der Waals interactions, which are captured using a Buckingham potential, and Coulomb interactions. The explicit form of the various force-field contributions and the potential parameters can be found in the literature.[43,44] There, it was also shown that the model well reproduces thermodynamic, structural, and dynamical properties of PPO melts.

All simulations are performed using the GROMACS software package.[45−49] We apply periodic boundary conditions and cut nonbonded interactions at a distance of 1.2 nm. The LINCS algorithm[46] is employed to constrain all bonds, and the particle-mesh Ewald technique[50] is used to calculate Coulomb interactions. A time step of $dt = 1$ fs is utilized. Prior to data acquisition, the systems are equilibrated at constant P and T, utilizing the Parrinello−Rahman barostat[51] and the Nosé−Hoover thermostat.[52−54] The equilibration times amount to multiples of τ.

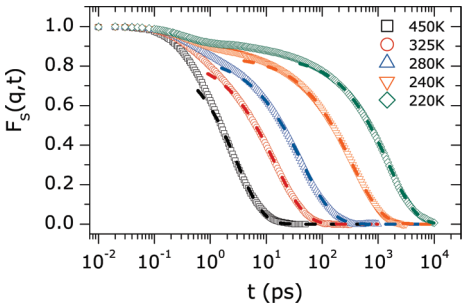

Figure 1. Incoherent intermediate scattering functions $F_s(q,t)$ for the oxygen atoms of PPO_4 at various temperatures ($q = 9.13$ nm^{-1}). The dotted lines are KWW fits of the long-time decays due to the α relaxation.

These equilibration periods enable adjustment of the density. Since dynamics is very sensitive to density, we use those configurations from the end of the equilibration runs as input for the subsequent production runs, for which the density is close to the average value. Data are acquired in the canonical ensemble, i.e., at constant V and T, by coupling the system to the Nosé−Hoover thermostat.

Results

Time Scale of the Segmental Relaxation. The properties of the α relaxation are analyzed based on incoherent intermediate scattering functions

$$F_s(q,t) = \langle \cos\{\mathbf{q}\cdot[\mathbf{r}(\tilde{t}_0 + t) - \mathbf{r}(\tilde{t}_0)]\}\rangle \quad (4)$$

which depend on the atomic displacements $[\mathbf{r}(\tilde{t}_0 + t) - \mathbf{r}(\tilde{t}_0)]$ during the time interval t. In our case of isotropic samples, the scattering functions only depend on the absolute value of the scattering vector $q = |\mathbf{q}|$, determining the length scale on which dynamics is monitored. Here, we show data for the oxygen atoms and use $q = 9.13$ nm^{-1}, corresponding to the first maximum of the intermolecular pair correlation function $g_{OO}(r)$.[44] The brackets $\langle ... \rangle$ denote the average over all oxygen atoms and various time origins $\tilde{t}_0$.

Figure 1 shows $F_s(q,t)$ for the example of PPO_4. At sufficiently low temperatures, the intermediate scattering functions show a pronounced temperature dependence and a two-step decay typical of glass-forming liquids.[55] Here, we focus on the α relaxation, which leads to the complete loss of correlation at long times. To quantify its slowdown upon cooling, we extract correlation times τ according to $F_s(q, t=\tau) = 1/e$. In Figure 2, we compare the temperature dependence of τ for all studied chain lengths N. As expected, the temperature dependence does not follow the Arrhenius law, but the Vogel−Fulcher−Tammann (VFT) law

$$\tau(T) = \tau_\infty \exp\left[\frac{C}{T - T_0}\right] \quad (5)$$

Then, a fragility plot is often used to compare the temperature dependence for different materials .[56] It shows $\log \tau$ as a function of reduced inverse temperature, T_{iso}/T, where T_{iso} is an isokinetic point; i.e., a temperature at which the materials exhibit the same value of τ, $T_{\text{iso}} = T(\tau = \text{constant})$. Exploiting that glass formers exhibit $\tau = 10^2$ s at the respective glass transition temperature, most experimental studies use $T_{\text{iso}} = T_g$ and define the fragility index

$$m = \left(\frac{\mathrm{d}\log\tau}{\mathrm{d}(T_g/T)}\right)_{T=T_g} \quad (6)$$

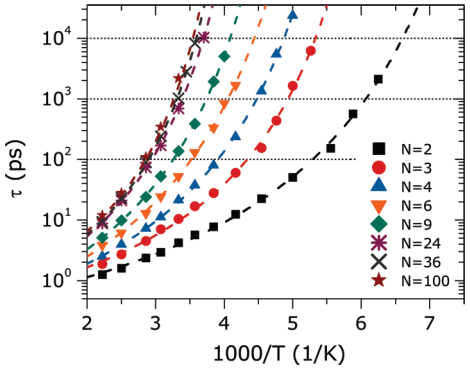

Figure 2. Temperature-dependent segmental relaxation times τ for PPO of various chain lengths N. The data were extracted from the incoherent scattering functions according to $F_s(q,t=\tau) = 1/e$. The dashed lines are VFT fits. The horizontal dotted lines mark the values $\tau = 0.1$ ns, $\tau = 1$ ns, and $\tau = 10$ ns.

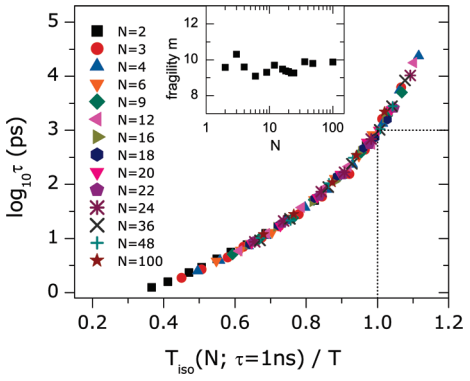

Figure 3. Segmental relaxation times τ for PPO of various chain lengths N as a function of T_{iso}/T. The dotted lines indicate that isokinetic points are defined according to $T_{iso} = T(\tau = 1$ ns). The inset shows the chain-length dependence of the fragility m at the reference temperature T_{iso} (see eq 6).

to measure deviations from Arrhenius behavior. Here, we define isokinetic points according to $T_{iso} = T(\tau = 10^{-9}$ s). In Figure 3, we show the resulting fragility plot for the studied PPO_N. Evidently, the data for all chain lengths nicely collapse onto a master curve, indicating that the fragility is independent of the molecular weight for our PPO model in the accessible temperature range. This result is confirmed when we inspect the inset of Figure 3, which shows the fragility $m(N)$ determined in analogy with eq 6 at $T = T_{iso}$. We see that $m \approx 9.5$ for all studied chain lengths $N = 2-100$. Of course, as a consequence of the VFT behavior, the present values of m, which reflect the temperature dependence well above T_g, are much smaller than the values found in experimental studies in the vicinity of the glass transition temperature, e.g., $m = 74$ for $PPO_{N\to\infty}$.[10]

To obtain further insights into the segmental motion, we study the chain-length dependence of the isokinetic points, $T_{iso}(N)$, mimicking the behavior of $T_g(N)$ in the accessible temperature range. Since the choice of the relaxation time may affect the results, three values of τ, namely, 0.1, 1, and 10 ns, are used to define isokinetic points. In Figure 4, we see that the shape of $T_{iso}(N)$ is independent of the value of τ, indicating that the analysis does not depend on the used value of the relaxation time, at least in the accessible time window. $T_{iso}(N)$ continuously increases when N increases; i.e., the data do not yield evidence for the existence of linear regimes. For further analysis, we fit $T_{iso}(N)$ to eqs 1 and 2.

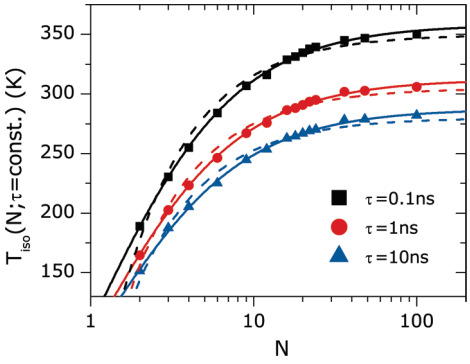

Figure 4. Chain-length dependence of the isokinetic point $T_{iso}(N) = T(N;\tau = \text{constant})$ for the indicated values of the segmental relaxation time τ. Dashed and solid lines are interpolations with eq 1 and eq 2, respectively.

Table 2. Parameters Obtained from Fitting eq 2 to Various Quantities Q Describing Structure and Dynamics of PPO (See Figure 9)

Q	Q_∞	K	N^*	K/Q_∞
T_{iso}	287 K	432 K	1.21	1.50
$1-\beta$	0.33	0.61	1.00	1.85
C	3.04	4.88	1.48	1.61
ρ	9.73 nm^{-3}	3.13 nm^{-3}	−0.50	0.32

We find that the interpolation of the curves is improved when using eq 2 rather than eq 1, but fit parameters $N^* \approx 1$ indicate that the deviations from the Fox−Flory approach are weak (see Table 2).

Nonexponentiality of the Segmental Relaxation. Next, we analyze the nonexponentiality of the α relaxation. To determine whether time−temperature superposition is fulfilled, we compare scaled scattering functions $F_s(q,t/\tau)$ for various temperatures in Figure 5. For the examples of PPO_4 and PPO_{36}, we see that time−temperature superposition holds at sufficiently low temperatures. Specifically, scaling does not work when vibrational motion interferes with segmental relaxation for $\tau \leq 100$ ps. Therefore, the high-temperature data are not included in Figure 5. To further study the nonexponentiality, we fit $F_s(q,t)$ with the Kohlrausch−Williams−Watts (KWW) function, $c\exp[-(t/\tau_{KWW})^{\beta}]$ (see Figure 1). The temperature dependence of the stretching parameter β is shown for various values of N in Figure 6a. Consistent with the results of our scaling analysis, cooling results in a decrease of β toward a plateau value, which is reached when τ exceeds about 100 ps. The existence of low-temperature plateaus of β provides further evidence that time−temperature superposition is fulfilled in this temperature range. However, the plateau value of β depends on the chain length, indicating that the nonexponentiality of the scattering functions varies with the molecular weight. To demonstrate this effect without any fitting procedure we compare scaled scattering functions $F_s(q,t/\tau)$ for various N in Figure 5c. For all N, we show curves characterized by $\tau \sim 1$ ns, ensuring that the respective low-temperature plateau of β is reached. Evidently, the decays are more stretched for longer chains. Figure 6b shows the low-temperature value of the stretching parameter as a function of the molecular weight. We see that $\beta(N)$ continuously decreases when the chain length increases until it saturates at $N = 30-40$.

The question arises whether the observed molecular-weight dependence of the nonexponentiality is the mere consequence of different mobilities of monomers at various positions along the chains. For example, one may expect that the mobility is higher for monomers at the end of a chain

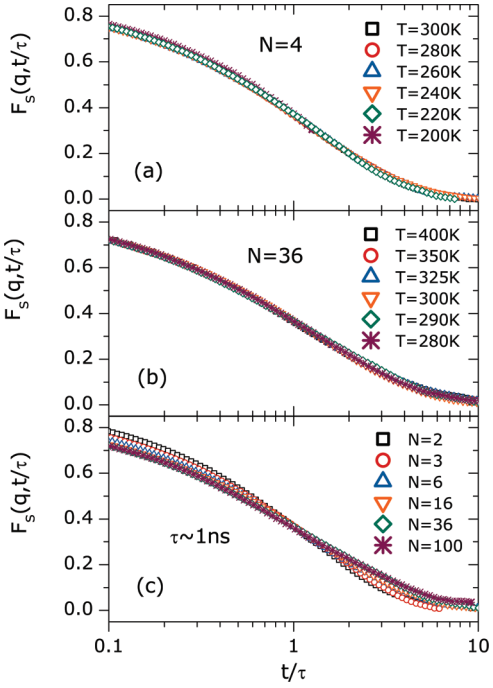

Figure 5. Scaled incoherent intermediate scattering functions $F_s(q,t/\tau)$ of PPO. Results at various temperatures are shown for (a) $N = 4$ and (b) $N = 36$. In panel (c), scattering functions, characterized by $\tau \sim 1$ ns, are compared for various chain lengths N.

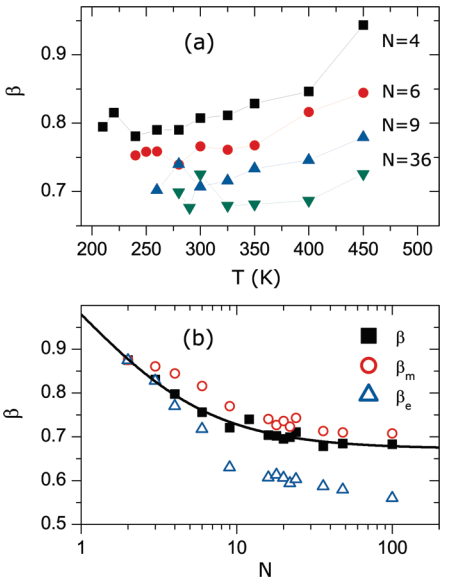

Figure 6. (a) Temperature dependence of the stretching parameter β for various values of N. (b) Chain-length dependence of the stretching parameter β, as obtained from averaging at sufficiently low temperatures. The line is a fit with a generalized Dobkowski equation, eq 9. The stretching parameters β_e and β_m characterize the respective stretching of the position-resolved scattering functions $f_s(q,t,\Delta n = 1)$ and $f_s(q,t,\Delta n = n_m)$ at sufficiently low temperatures; i.e., they are a measure for the nonexponentiality of monomer dynamics at the end and in the middle of a polymer chain.

than for monomers in the middle of a chain, as observed in MDS of poly(methylene) melts.[57] Then, longer chains, which comprise different types of monomers, would show higher nonexponentiality since the observed relaxation is a superposition of the respective dynamical behaviors. To quantify the effect, we separately calculate the incoherent scattering functions for the oxygen atoms at different positions Δn

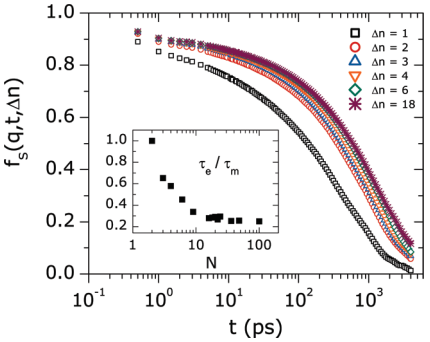

Figure 7. Position-resolved incoherent intermediate scattering functions $f_s(q,t,\Delta n)$ for the oxygen atoms at different distances Δn from the nearest chain end of PPO_{36}; see text for details ($q = 9.13$ nm^{-1}, $T = 300$ K). The inset shows the chain-length dependence of the ratio of the relaxation times τ_e and τ_m, which are defined as $f_s(q,\tau_e,\Delta n = 1) = 1/e$ and $f_s(q,\tau_m,\Delta n = n_m) = 1/e$, respectively.

within the chains. Here, Δn is the distance of a monomer from the nearest chain end, starting with $\Delta n = 1$ for the end groups. Figure 7 shows the position-resolved scattering functions $f_s(q,t,\Delta n)$ for PPO_{36} at 300 K. We see that the decays shift to longer times when starting from the chain end and moving toward the chain center until saturation is observed at $\Delta n \approx 6$. Thus, there are diverse mobilities along the chains so that a superposition of the respective contributions enhances the nonexponentiality. To study the relevance of this superposition effect, we compare the time constants τ_e and τ_m describing the relaxation behaviors of terminal monomers ($\Delta n = 1$) and middle monomers ($\Delta n = n_m$), respectively. Here, $n_m = N/2$ for even N and $n_m = (N+1)/2$ for odd N. In the inset of Figure 7, the N dependence of the ratio τ_e/τ_m is displayed. For $N = 2$, monomers exhibiting distinguishable dynamical behaviors along the chain do not exist and, hence, $\tau_e = \tau_m$. When the chains become longer, the dynamics at the ends of the chains increasingly decouples from that in the middle of the chains so that τ_e/τ_m decreases. Eventually, the dynamics of terminal monomers is by about a factor of 4 faster than that of the middle monomers in the limit of long chains.

This analysis reveals that the nonexponentiality is affected by the diversity of the mobility along the chains. However, the phenomenon is not a simple superposition effect, as can be inferred from an analysis of the stretching of the position-resolved scattering functions, which are not affected by mobility differences along the chains. The stretching parameters β_e and β_m, which describe the nonexponentiality of $f_s(q,t,\Delta n = 1)$ and $f_s(q,t,\Delta n = n_m)$, respectively, are included in Figure 6b. We see that, for terminal and middle monomers, the scattering functions are more stretched for long chains than for short chains, suggesting that the nonexponentiality of the segmental relaxation is enhanced by chain connectivity at all positions along the chains.

Chain Conformation and Monomer Density. The question arises to which extent the molecular-weight dependence of the segmental relaxation can be traced back to structural changes. To tackle this question, we study the chain conformation and the monomer density as a function of N. Information about the chain conformation is available when we study the relative orientation of bond vectors along the polymer backbone. For this purpose, we define the bond−bond correlation function

$$B(\delta n) = \langle \mathbf{e}_{n_m} \cdot \mathbf{e}_{n_m+\delta n} \rangle \qquad (7)$$

Here, $\mathbf{e}_i$ is the unit vector connecting the oxygen atoms of the monomers i and $i+1$ along a chain. Figure 8 shows $B(\delta n)$ for

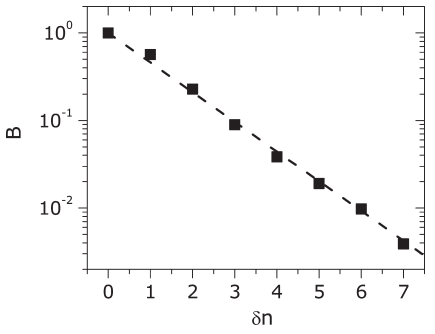

Figure 8. Bond−bond correlation function $B(\delta n)$ for PPO_{36} at $T = 450$ K (see eq 7). The dashed line is a fit with an exponential decay.

PPO_{36} at $T = 450$ K, but we ensured that the results do not depend on the value of N for sufficiently long chains. We see that the orientational correlation of two segments diminishes exponentially with the number of monomers between these segments, as expected for Gaussian chains.[58] Thus, fitting the data with an exponential decay, $\exp(-\delta n/\delta n_{ps})$, allows us to determine the persistence length according to $l_{ps} = a\delta n_{ps}$, where $a = 3.19$ Å is the intramolecular oxygen−oxygen distance. The analysis yields $\delta n_{ps} = 1.28$ and $l_{ps} = 4.08$ Å. While our finding of an exponential decay of the bond−bond correlation function is consistent with textbook knowledge about Gaussian chains,[58] power-law decays were reported for dense polymer solutions.[59]

The characteristic ratio C is another source of information about chain conformation. A decrease of the molecular weight results in a crossover from Gaussian behavior to non-Gaussian behavior,[60] which manifests itself in a chain-length dependence of the characteristic ratio, $C(N)$. To monitor this crossover for the PPO model, we determine the mean squared end-to-end distance $\langle R_e^2(N)\rangle$ and calculate the characteristic ratio according to

$$C(N) = \frac{\langle R_e^2(N)\rangle}{(N-1)a^2} \tag{8}$$

In Figure 9, it is evident that $C(N)$ converges toward the long-chain limit $C_\infty \approx 3.04$, being a measure of chain stiffness. Using the relation $C_\infty = 2l_{ps}/a$,[61] the characteristic ratio can also be calculated from the above determined persistence length. This calculation yields $C_\infty = 2.56$, in reasonable agreement with the value obtained from the end-to-end distances. Inspection of Figure 9 reveals that the properties of the segmental relaxation cease to change when the chain conformation starts to obey Gaussian statistics at chain lengths $N_G = 30-40$, consistent with observations in experimental work.[13]

In addition, Figure 9 shows the number density of the monomers, ρ, as a function of N for $T = 300$ K. We see that not only $C(N)$ but also $\rho(N)$ shows a chain-length dependence that is highly comparable to that of the time constant τ and of the nonexponentiality parameter $1-\beta$ of the segmental relaxation, suggesting a close relation between structure and dynamics. Since eq 2 enabled a good interpolation of $T_{iso}(N)$, we further investigate a potential relation by fitting also the other quantities Q to ($Q = 1-\beta$, C, ρ):

$$Q(N) = Q_\infty - \frac{K}{N+N^*} \tag{9}$$

In Figure 9, we see that this approach allows us a good interpolation of all data. The resulting fit parameters are compiled in Table 2. For a straightforward comparison of

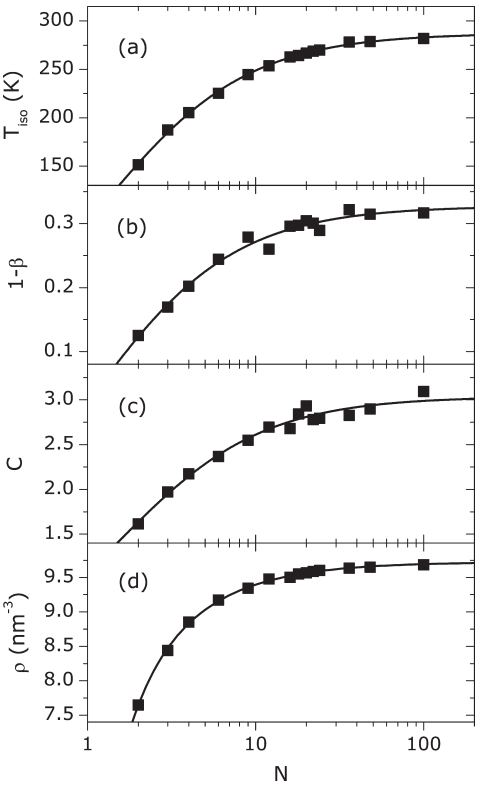

Figure 9. Chain-length dependence of dynamical and structural properties of PPO: (a) isokinetic point $T_{iso}(N)$ for $\tau = 10$ ns (see Figure 4), (b) nonexponentiality parameter $1-\beta(N)$ (see Figure 6), (c) characteristic ratio $C(N)$ at $T = 450$ K, and (d) number density of monomers $\rho(N)$ at $T = 450$ K. The lines are fits to eq 9.

the chain-length dependence, it is useful to consider the normalized quantities Q/Q_∞ and, hence, the scaled parameter K/Q_∞. Inspecting Table 2, it is evident that the studied dynamical and structural properties of the model polymer show a very similar dependence on the molecular weight. For the number density, we find somewhat smaller values of N^* and K/Q_∞, but the behavior is still comparable. These correlations imply that the segmental relaxation is strongly affected by the chain conformation. To investigate in more detail to which extent excess free volume in the vicinity of end groups leads to not only a lower monomer density but also a faster structural relaxation when the molecular weight is reduced, we apply free-volume theory in the next section.

Free-Volume Approach. In seminal works,[40,41] Doolittle found that the viscosity η and, thus, the relaxation time τ are related to the relative free volume

$$\frac{v_f}{v_0} = \frac{v_T - v_0}{v_0} \tag{10}$$

Here, v_T and v_0 are the volumes per monomer at a finite temperature T and absolute zero, respectively. Explicitly, an exponential relation was proposed, leading to

$$\ln \tau = \ln A + B\frac{v_0}{v_f} \tag{11}$$

If chain ends cause excess free volume and, hence, v_f is higher for shorter chains, τ will increase when N increases, consistent with the observed molecular-weight dependence of T_g. Motivated by these arguments, we determine the volume per monomer, $v = 1/\rho$, for all studied N and T. In Figure 10, we

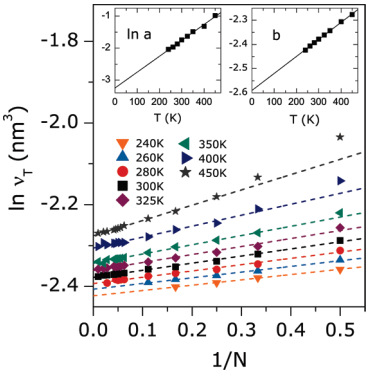

Figure 10. Volume per monomer, v_T, as a function of the chain length N for the indicated temperatures. The dashed lines are fits to eq 12. The insets show the temperature dependence of the fit parameters ln(a) and b. The lines are interpolations with linear functions; see text for details.

see that the chain-length dependence of v_T is well described by

$$\ln v_T(N) = \frac{a(T)}{N} + b(T) \tag{12}$$

at the studied temperatures, as was proposed by Doolittle. Therefore, we further follow his approach to determine v_0 and, thus, the relative free volume, from extrapolation of v_T to absolute zero. Specifically, we fit the temperature dependence of a and b with $\ln a = c_1T + c_2$ and $b = c_3T + c_4$. In the insets of Figure 10, we see that Doolittle's approach yields good interpolations. The fit parameters are $c_1 = 5.0 \times 10^{-3}$ K^{-1}, $c_2 = -3.2$, $c_3 = 7.0 \times 10^{-4}$ K^{-1}, and $c_4 = 2.6$, when volumes are in nm^3. On the basis of these parameters, $v_T(N)$ can be calculated for all T and N, providing access to the relative free volume $v_f/v_0(T,N)$. Of course, the present method does not enable a rigorous determination of the relative free volume, which is difficult in any case. In particular, we neglect that factors other than thermal contraction can lead to a decrease in the free volume upon cooling.[62]

Figure 11 presents a test of the free-volume theory. In panel (a), we show log τ as a function of the inverse of the relative free volume, $(v_f/v_0)^{-1}$. While comparable behavior is observed for $N \geq 20$, the data for shorter chains do not collapse onto a master curve. Furthermore, we do not find a linear increase, as predicted by eq 11, but rather a superlinear increase, suggesting a divergence of the relaxation time at a finite value of the relative free volume. Simultaneously fitting the curves for $N \geq 20$ to a VFT-like behavior (see Figure 11) yields evidence for a divergence at $(v_f/v_0)_{min} = 0.131$. These results imply that the polymer chains cannot access the whole free volume determined within Doolittle's approach. Consistently, previous work argued that a portion of the excess volume $v_T - v_0$ stems from anharmonic vibration and cannot be redistributed during α relaxation.[63,64] Therefore, we consider the reduced relative free volume

$$\left(\frac{v_f}{v_0}\right)_{red} = \frac{v_f}{v_0} - \left(\frac{v_f}{v_0}\right)_{min} \tag{13}$$

Here, we use $(v_f/v_0)_{min} = 0.131$ for all chain lengths. In panel (b), we see that log τ linearly depends on the inverse of the thus defined reduced relative free volume for all studied N, as predicted by free-volume theory. However, the slope of the curves increases with increasing chain lengths until it saturates at $N = 30-40$ (see the inset of Figure 11). The observed slopes correspond to values 0.3−1.0 for parameter B in

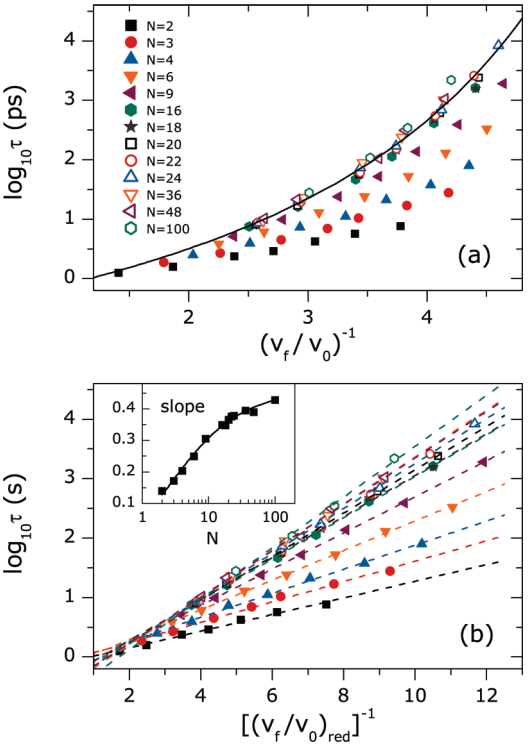

Figure 11. Test of the free-volume theory: (a) log τ as a function of the inverse of the relative free volume, $(v_f/v_0)^{-1}$. The solid line is a fit to $a_1 + a_2/(v_0/v_f - a_3)$, which yields $a_3 = 7.61$, suggesting a divergence of the segmental relaxation time at $(v_f/v_0)_{min} = 0.131$. (b) log τ as a function of the inverse of the reduced relative free volume, $[(v_f/v_0)_{red}]^{-1}$, which is defined in eq 13. The dashed lines are fits to a linear function. The inset shows the resulting slopes as a function of the chain length N. The solid line is an interpolation using eq 14.

eq 11, in harmony with its interpretation as overlap parameter.[63,64] Consistent with the present findings, Doolittle reported that the dependence of log τ on v_0/v_f differs for paraffins of diverse molecular weights. When we follow his approach and fit the chain-length dependent slope to

$$b_1 \exp\left(-\frac{b_2}{N^{b_3}}\right) \tag{14}$$

we obtain $b_1 = 0.46$, $b_2 = 2.1$, and $b_3 = 0.71$. However, the quality of the interpolation is not reduced when using other fitting functions, e.g., eq 9.

Discussion

For a PPO model, we found that a VFT law well describes the temperature dependence of the segmental relaxation time τ for chain lengths $N = 2-100$. All data nicely collapse onto a master curve when plotted on a reduced temperature scale, i.e., in a fragility plot.[56] Hence, the fragility is independent of the degree of polymerization in the accessible temperature range $T > 1.2T_g$. Consistently, no dependence of the fragility on the molecular weight was observed in experimental work on PPO in the vicinity of T_g.[65,66] In experimental studies on other polymers, a molecular-weight-independent fragility was found for some materials,[8,10,67,68] while the fragility of most materials substantially varies when the chain length is increased in the oligomeric regime.[7,8,10,11,68−72] It is a widespread opinion that the mechanism for the α relaxation of viscous liquids changes when approaching T_g, e.g., that activated hopping processes are unimportant above a crossover temperature T_c, while they are important below T_c. At the present, it is unclear to which extent this

change of mechanism affects the molecular-weight dependence of the fragility and, hence, whether computational results above T_c can directly be compared with experimental findings below T_c, although the present computational and previous experimental studies on PPO yield a coherent picture. For example, it was proposed to use separate definitions of fragility for each regime.[73] However, one may hope that fragilities defined in different temperature ranges are related. To shed some light on this question in future studies, it may be interesting to construct fragility plots of experimental data using reference temperatures $T > 1.2T_g$, comparable to that of the present computational study.

To further ascertain the molecular-weight dependence of the segmental relaxation, we determined isokinetic points $T_{iso}(N)$ from the criterion that the relaxation time τ has a specific value at these temperatures. Then, the curves $T_{iso}(N)$ can be expected to mimic the dependence of T_g on the degree of polymerization. In the accessible temperature range, we observed that T_{iso} is a smooth function of N. Specifically, the data are well described by a modification[5] of the Fox−Flory equation (see eq 2). Thus, the present results are consistent with the continuous molecular-weight dependence of the segmental relaxation reported in some experimental studies,[6−10] including a smooth variation of T_g as a function of N found for PPO,[66] while they do not yield evidence for the existence of linear regions of $T_{iso}(N)$, which were reported for $T_g(N)$ in other experimental approaches.[11,12] We note that a peculiar behavior of $T_g(N)$ was observed for poly(propylene glycol) (PPG), where the CH_3 end groups of PPO are replaced by OH end groups.[74]

Scaling and fitting analyses revealed that the segmental relaxation obeys time−temperature superposition at sufficiently low temperatures, where it does not interfere with vibrational motion. Comparing the shape of the decays in this temperature range, we found that the curves are more stretched for longer chains and, thus, the KWW stretching parameter β decreases when N increases. Consistently, experimental work on PPG reported enhanced nonexponentiality for higher molecular weights,[69] while the stretching was found to be independent of N for other polymers.[7,8,11] In the present case, the more pronounced nonexponentiality for longer chains results from both a diversity of monomer mobilities along the backbone, i.e., faster relaxation of monomers near chain ends, and from a molecular-weight dependent stretching at all monomer positions. For the temperature range in vicinity of T_g, it was established that the stretching parameter β is correlated with the fragility m such that large m are usually associated with small β.[75] Here, we observed that the stretching does and the fragility does not depend on N, indicating that β and m are not correlated for the PPO model well above T_g, suggesting that a potential relation between these quantities may be restricted to highly viscous liquids where dynamics is dominated by the potential energy landscape. However, exceptions to the correlation were also observed for polymer melts near T_g.[7,11]

Interestingly, we found that the molecular-weight dependence of the segmental motion is very similar to that of the characteristic ratio C, implying a close relation between dynamics and structure. In particular, the time constant and the nonexponentiality of the segmental relaxation saturate at chain lengths $N_G = 30-40$, at which the characteristic ratio reaches the limiting value C_∞. Hence, the chain-length dependence of the segmental relaxation ceases when Gaussian chain conformation is established, consistent with results of previous experimental[9,13] and theoretical[76] approaches. By contrast, the molecular-weight dependence of the segmental relaxation vanishes before the entanglement limit is reached at $N_E \approx 90$.[77]

Since it is often argued that the excess free volume in the vicinity of chain ends is at the origin of the chain-length dependence of the α relaxation and, thus, of T_g, we studied whether free-volume theory captures the present observations. Using Doolittle's approach to determine the occupied volume per monomer v_0 and the free volume per monomer v_f, we did not observe the theoretical prediction of a linear relationship between $\log \tau$ and v_0/v_f. However, a linear relationship resulted for all studied chain lengths N when reducing the relative free volume by about 13%, in qualitative agreement with previous arguments.[63,64] Then, the slope of the lines increases with increasing molecular weight for $N < N_G$ while it is independent of the degree of polymerization for larger $N \geq N_G$. These results imply that the availability of free volume does play a role for the segmental relaxation, but free-volume theory does not capture all the subtle effects. For example, one may speculate that, due to the chain connectivity and the cooperative nature of the dynamics, relaxation requires the availability of free volume for several rather than one polymer segment, where the number of the involved segments may depend on N and T.

Conclusions

Performing MDS for PPO, we investigated the dependence of the segmental (α) relaxation on the molecular weight. For this purpose, incoherent intermediate scattering functions $F_s(q,t)$ of the oxygen atoms were analyzed for a scattering vector corresponding to the intermolecular oxygen−oxygen distance. The analysis showed that the fragility is independent of the chain length N and that the properties of the α relaxation, e.g., the relaxation time τ, are smooth functions of N. These results indicate that an increase of the degree of polymerization does not lead to qualitative changes of the glass transition phenomenon in the oligomeric regime. The molecular-weight dependence of the α relaxation is very similar to that of the characteristic ratio, implying a close relation between segmental motion and chain conformation.

List of Symbols

N = number of monomers of a chain
N_R = number of monomers of a Rouse unit
N_E = number of monomers between entanglements
τ = segmental relaxation time
β = stretching parameter
T_{iso} = isokinetic point
F_s = incoherent intermediate scattering function
f_s = position-resolved incoherent intermediate scattering function
τ_e = segmental relaxation time of terminal monomers
β_e = stretching parameter of terminal monomers
τ_m = segmental relaxation time of middle monomers
β_m = stretching parameter of middle monomers
Δn = distance of a monomer from the nearest chain end
l_{ps} = persistence length
a = intramolecular oxygen−oxygen distance
C = characteristic ratio
ρ = number density of monomers
v_T = volume per monomer at temperature T
v_0 = volume per monomer at temperature $T = 0$ K
m = fragility index

References and Notes

(1) Fox, T. G.; Flory, P. J. *J. Appl. Phys.* **1950**, *21*, 581–591.
(2) Fox, T. G.; Flory, P. J. *J. Polym. Sci.* **1954**, *14*, 351–319.
(3) *Amorphous Materials*; Douglas, R. W., Ellis, B., Eds.; Wiley-Interscience: New York, 1972.
(4) Kim, Y. W.; Park, J. T.; Koh, J. H.; Min, B. R.; Kim, J. H. *Polym. Adv. Technol.* **2008**, *19*, 944–946.
(5) Dobkowski, Z. *Eur. Polym. J.* **1982**, *18*, 563–567.

(6) Marchionni, G.; Ajroldi, G.; Pezzin, G. *Eur. Polym. J.* **1988**, *24*, 1211–1216.
(7) Santangelo, P. G.; Roland, C. M. *Macromolecules* **1998**, *31*, 4581–4585.
(8) Robertson, C. G.; Roland, C. M. *J. Polym. Sci., Part B: Polym. Phys.* **2004**, *42*, 2604–2611.
(9) Ding, Y.; Kisliuk, A.; Sokolov, A. P. *Macromolecules* **2004**, *37*, 161–166.
(10) Ding, Y.; Novikov, V. N.; Sokolov, A. P.; Cailliaux, A.; Dalle-Ferrier, C.; Alba-Simionesco, C.; Frick, B. *Macromolecules* **2004**, *37*, 9264–9272.
(11) Hintermeyer, J.; Herrmann, A.; Kahlau, R.; Goiceanu, C.; Rössler, E. A. *Macromolecules* **2008**, *41*, 9335–9344.
(12) Cowie, J. M. G. *Eur. Polym. J.* **1975**, *11*, 297–300.
(13) Agapov, A. L.; Sokolov, A. P. *Macromolecules* **2009**, *42*, 2877–2878.
(14) Binder, K.; Baschnagel, J.; Paul, W. *Prog. Polym. Sci.* **2003**, *28*, 115–172.
(15) Baschnagel, J.; Varnik, F. *J. Phys.: Condens. Matter* **2005**, *17*, R851–R953.
(16) Paul, W.; Smith, G. D. *Rep. Prog. Phys.* **2004**, *67*, 1117–1185.
(17) Smith, G. D.; Bedrov, D. *J. Polym. Sci., Part B: Polym. Phys.* **2007**, *45*, 627–643.
(18) Baschnagel, J.; Binder, K.; Doruker, P.; Gusev, A. A.; Hahn, O.; Kremer, K.; Mattice, W. L.; Müller-Plathe, F.; Murat, M.; Paul, W.; Santos, S.; Suter, U. W.; Tries, V. *Adv. Polym. Sci.* **2000**, *152*, 41–156.
(19) Glotzer, S. C.; Paul, W. *Annu. Rev. Mater. Res.* **2002**, *32*, 401–436.
(20) Kremer, K.; Grest, G. S. *J. Chem. Phys.* **1990**, *92*, 5057–5086.
(21) Smith, S. W.; Hall, C. K.; Freeman, B. D. *Phys. Rev. Lett.* **1995**, *75*, 1316–1319.
(22) Mondello, M.; Grest, G. S., III; E. B., W.; Peczak, P. *J. Chem. Phys.* **1998**, *109*, 798–805.
(23) Harmandaris, V. A.; Mavrantzas, V. G.; Theodorou, D. N. *Macromolecules* **1998**, *31*, 7934–7943.
(24) Padding, J. T.; Briels, W. J. *J. Chem. Phys.* **2002**, *117*, 925–943.
(25) Harmandaris, V. A.; Doxastakis, M.; Mavrantzas, V. G.; Theodorou, D. N. *J. Chem. Phys.* **2002**, *116*, 436–446.
(26) Lee, S. H.; Chang, T. *Bull. Korean Chem. Soc.* **2003**, *24*, 1590–1598.
(27) Harmandaris, V. A.; Mavrantzas, V. G.; Theodorou, D. N.; Kröger, M.; Ramirez, J.; Öttinger, H. C.; Vlassopouos, D. *Macromolecules* **2003**, *36*, 1376–1387.
(28) Barbieri, A.; Prevosto, D.; Lucchesi, M.; Leporini, D. *J. Phys.: Condens. Matter* **2004**, *16*, 6609–6618.
(29) Karayiannis, N. C.; Mavrantzas, V. G.; Theodorou, D. N. *Macromolecules* **2004**, *37*, 2978–2995.
(30) Bulacu, M.; van der Giessen, E. *J. Chem. Phys.* **2005**, *123*, 114901/1–13.
(31) Depa, P. K.; Maranas, J. K. *J. Chem. Phys.* **2007**, *126*, 054903/1–8.
(32) Zhang, J.; Liang, Y.; Yan, J.; Lou, J. *Polymer* **2007**, *48*, 4900–4905.
(33) Logotheti, G. E.; Theodorou, D. N. *Macromolecules* **2007**, *40*, 2235–2245.
(34) Vallee, R. A. L.; Paul, W.; Binder, K. *J. Chem. Phys.* **2010**, *132*, 034901/1–9.
(35) *Solid Polymer Electrolytes*; Gray, F. M., Ed.; Wiley: New York, 1991.
(36) Vogel, M.; Torbrügge, T. *J. Chem. Phys.* **2006**, *125*, 054905/1–10.
(37) Vogel, M.; Torbrügge, T. *J. Chem. Phys.* **2006**, *125*, 164910/1–13.
(38) Vogel, M.; Torbrügge, T. *J. Chem. Phys.* **2007**, *126*, 204902/1–15.
(39) Vogel, M. *Macromolecules* **2008**, *41*, 2949–2958.
(40) Doolittle, A. K. *J. Appl. Phys.* **1951**, *22*, 1471–1475.
(41) Doolittle, A. K. *J. Appl. Phys.* **1951**, *23*, 236–239.
(42) Cohen, M. H.; Turnbull, D. *J. Chem. Phys.* **1959**, *31*, 1164–1169.
(43) Smith, G. D.; Borodin, O.; Bedrov, D. *J. Phys. Chem. A* **1998**, *102*, 10318–10323.
(44) Wahnstrom, G.; Ahlstrom, P.; Borodin, O.; Wensink, E. J. W.; Carlsson, P.; Smith, G. D. *J. Chem. Phys.* **2000**, *112*, 10669–10679.
(45) Berendsen, H. J. C.; van der Spoel, D.; van Drunen, R. *Comput. Phys. Commun.* **1995**, *91*, 43–56.
(46) Hess, B.; Bekker, H.; Berendsen, H. J. C.; Fraaije, J. G. E. M. *J. Comput. Chem.* **1997**, *18*, 1463–1472.
(47) Lindahl, E.; Hess, B.; van der Spoel, D. *J. Mol. Model.* **2001**, *7*, 306–317.
(48) van der Spoel, D.; Lindahl, E.; Hess, B.; Groenhof, G.; Mark, A. E.; Berendsen, H. J. C. *J. Comput. Chem.* **2005**, *26*, 1701–1718.
(49) Hess, B.; Kutzner, C.; van der Spoel, D.; Lindahl, E. *J. Chem. Theory Comput* **2008**, *4*, 435–447.
(50) Essman, U.; Perera, L.; Berkowitz, M. L.; Darden, T.; Lee, H.; Pedersen, L. G. *J. Chem. Phys.* **1995**, *103*, 8577–8593.
(51) Parrinello, M.; Rahman, A. *J. Appl. Phys.* **1981**, *52*, 7182–7190.
(52) Nosé, S. *Mol. Phys.* **1984**, *52*, 255–268.
(53) Nosé, S. *J. Chem. Phys.* **1984**, *81*, 511–519.
(54) Hoover, W. G. *Phys. Rev. A* **1985**, *31*, 1695–1697.
(55) Götze, W.; Sjogren, L. *Rep. Prog. Phys.* **1992**, *55*, 241–376.
(56) Angell, C. A. *J. Non-Cryst. Solids* **1991**, *131*−*133*, 13–31.
(57) Smith, G. D.; Yoon, D. Y.; Zhu, W.; Ediger, M. D. *Macromolecules* **1994**, *27*, 5563–5569.
(58) *Statistical Physics of Macromolecules*; Grosberg, A. Y., Khokhlov, A. R., Eds.; American Institute of Physics: New York, 1994.
(59) P.Wittmer, J.; Meyer, H.; Baschnagel, J.; Johner, A.; Obukhov, S.; Mattioni, L.; Müller, M.; Semenov, A. N. *Phys. Rev. Lett.* **2004**, *93*, 147801/1–4.
(60) *Statistical Mechanics of Chain Molecules*; Flory, P. J., Ed.; Interscience: New York, 1969.
(61) *The Physics of Polymers*; Strobl, G., Ed.; Springer: Heidelberg, 2007.
(62) Xiao, D.; Rajian, J. R.; Cady, A.; Li, S.; Bartsch, R. A.; Quitevis, E. L. *J. Phys. Chem. B* **2007**, *111*, 4669–4677.
(63) Turnbull, D.; Cohen, M. H. *J. Chem. Phys.* **1961**, *34*, 120–125.
(64) Vrentas, J. S. *J. Appl. Polym. Sci.* **1978**, *22*, 2325–2339.
(65) Roland, C. M.; Ngai, K. L. *Macromolecules* **1992**, *25*, 5765–5768.
(66) Mattsson, J.; Bergman, R.; Jacobsson, P.; Börjesson, L. *Phys. Rev. Lett.* **2005**, *94*, 165701/1–4.
(67) Roland, C. M.; Ngai, K. L. *Macromolecules* **1996**, *29*, 5747–5750.
(68) Pawlus, S.; Kunal, K.; Hong, L.; Sokolov, A. P. *Polymer* **2008**, *49*, 2918–2923.
(69) Leon, C.; Ngai, K. L.; Roland, C. M. *J. Chem. Phys.* **1999**, *110*, 11585–11591.
(70) Casalini, R.; Roland, C. M.; Capaccioli, S. *J. Chem. Phys.* **2007**, *126*, 184903/1–11.
(71) Schröter, K.; Reissig, S.; Hempel, E.; Beiner, M. *J. Non-Cryst. Solids* **2007**, *353*, 3796–3983.
(72) Elfadl, A. A.; Herrmann, A.; Hintermeyer, J.; Petzold, N.; Novikov, V. N.; Rössler, E. A. *Macromolecules* **2009**, *42*, 6816–6817.
(73) Dudowicz, J.; Freed, K. F.; Douglas, J. F. *J. Phys. Chem. B* **2005**, *109*, 21350–21356.
(74) Gainaru, C.; Hiller, W.; Böhmer, R. *Macromolecules* **2010**, *43*, 1907–1914.
(75) Böhmer, R.; Ngai, K. L.; Angell, C. A.; Plazek, D. J. *J. Chem. Phys.* **1993**, *99*, 4201–4209.
(76) Saltzman, E. J.; Schweizer, K. S. *J. Phys.: Condens. Matter* **2007**, *19*, 205123/1–13.
(77) Gainaru, C.; Böhmer, R. *Macromolecules* **2009**, *42*, 7616–7618.